31st International Conference Nuclear Energy for New Europe
NENE 2022 September 12-15 PORTOROŽ SLOVENIA

Calculation of the QUENCH-02 Experiment with the ASYST Code Including the Uncertainty Evaluation

Siniša Šadek, Renato Pavlinac, Karlo Ivanjko, Davor Grgić
University of Zagreb, Faculty of electrical engineering and computing
Unska 3
10000 Zagreb, Croatia
sinisa.sadek@fer.hr, renato.pavlinac@fer.hr, karlo.ivanjko@fer.hr, davor.grgic@fer.hr

ABSTRACT

Uncertainties in the safety assessment of nuclear facilities are the result of random and systematic errors: variabilities in the values of the variables describing the system and its initial and boundary conditions, and the lack of precision of calculation models. Varying the input variables will cause the results of the calculation to be scattered depending on the predefined confidence level. The ASYST code, developed as part of an international nuclear technology ASYST Development and Training Program (ADTP) managed by Innovative Systems Software (ISS), is used to perform an uncertainty analysis of the QUENCH-02 experiment conducted at the Karlsruhe Institute of Technology. The code uses a probabilistic methodology based on the propagation of input uncertainties.

The QUENCH facility consists of 21 fuel rod simulators, 20 of which are electrically heated. The aim of the QUENCH experiments is to examine hydrogen source term and the behaviour of the fuel rod cladding during core reflood, in a typical PWR reactor. The QUENCH-02 experiment did not have a pre-oxidation phase; thus the objective was the investigation of PWR fuel rods behaviour with little oxidation. The experiment consisted of a heatup phase to temperature of 900 K, a transient phase in which the temperature rose to approximately 2300 K, and a quenching phase with mass flow of water 40-50 g/s.

For selected input parameters, such as steam/water flow, electric power and other relevant boundary conditions, it is necessary to define their probability density functions. Input databases are then prepared for individual calculations based on the selected level and confidence interval. The number of calculations is large enough to ensure at least 95% coverage of expected output results and uncertainty limits. The results of the calculations are compared with the experimental measurements. The Pearson correlation coefficient is used to obtain correlation between the input uncertain parameters and the output data. Sensitivity analysis covered the influence of variations in the heater electric power on the hydrogen production and the maximum cladding temperature.

1 INTRODUCTION

The Integrated Uncertainty Analysis (IUA) module introduced into the code ASYST [1] allows users to quantify the influence of uncertainties in the experimental conditions and important physical models/correlations. The calculation of the experiment QUENCH-02 [2] was used to test the IUA option, to determine the critical input parameters and to make a sensitivity analysis of the calculation results.

The ASYST code is a severe accident code developed to analyse behaviour of nuclear power plants and experimental facilities. It uses best-estimate thermal hydraulic two-fluid, non-

equilibrium, non-homogenous models, models and correlations for calculation of in-vessel severe accident progression and the finite element model for thermal analysis of the reactor vessel lower head. For the purpose of application in CORA [3] and QUENCH experiments, a dedicated model was developed to simulate electric tungsten heaters coated with zirconium alloy cladding. The IUA package was previously mostly used for analyses of nuclear power plants [4-7], but was once used also for the analysis of the QUENCH-06 experiment [8] conducted in the same QUENCH test facility as the experiment QUENCH-02. That analysis was focused at the influence of uncertainties in the correlations for Zircaloy oxidation, the tungsten heater element resistances, the convective heat transfer coefficients and the thermal conductivity of the ZrO_2 thermal insulation of the test bundle.

The QUENCH nodalization was adapted from the RELAP5/SCDAPSIM model [9, 10] of the QUENCH facility used in the calculation of QUENCH-06 and QUENCH-11 experiments, respectively. It faithfully represents the geometry of the facility, experimental conditions, heat losses, properties of electrically heated rods, zirconia insulating shroud, inlet plenum, outlet plenum, initial and boundary conditions.

2 QUENCH FACILITY AND THE EXPERIMENT

2.1 Description of the QUENCH Test Section

The QUENCH facility (Figure 1) consists of the test bundle with fuel rod simulators, the electric power supply, steam, argon, water supply systems, measurements devices, process control and data acquisition systems.

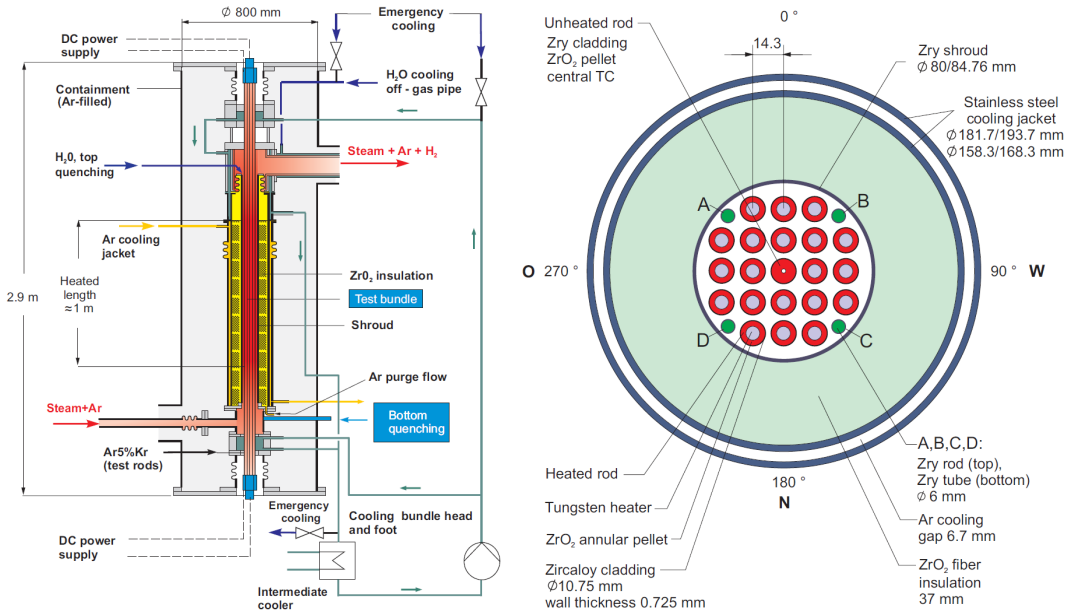

Figure 1: QUENCH facility and the test bundle

There are 21 fuel rod simulators (20 heated and one unheated rod) within the bundle and four Zircaloy corner rods. Fuel rod simulators consist of central tungsten heater, ZrO_2 annular pellets and Zircaloy cladding with dimensions equal to cladding of PWR nuclear power plant fuel rods. This way, real conditions like in the power plant are ensured during heating, oxidation

and quenching of the overheated, partially or completely oxidized, reactor core, with emphasis on the fuel rod cladding behaviour. The heated section is approximately 1 m high. Tungsten heaters are connected to power supply by molybdenum and copper electrodes on the top and the bottom of the tungsten elements. The bundle thermal insulation is provided by using the ZrO_2 fibre insulation mounted within the inner Zircaloy and outer stainless steel tube. There is no insulation above the heated zone and the whole space between the tubes is filled with argon. The outer tube is cooled with flowing argon in the heated zone and with water above it.

2.2 QUENCH-02 Experimental Setup

The QUENCH-02 experiment was performed in the QUENCH facility on July 7, 1998 at the Karlsruhe Institute of Technology. The bundle was heated by a series of stepwise increases of electrical power from the room temperature to nearly 900 K in the atmosphere of flowing argon and steam, 3 g/s each at temperature 660-680 K and pressure 200 kPa. At the end of the thermal stabilization period, the bundle heating power was ramped from 3.75 kW to 16.35 kW (Figure 2a), the process lasting for 2100 s. This phase lasted for a relatively short time to ensure little oxidation of the cladding before water flooding, which was the intention of the experiment. The steam supply was then turned off and the quench water at temperature 293 K was being injected at a flow rate 87 g/s for 20 s and then at 46 g/s for 233 s (Figure 2b). With the start of the quench water injection, the electric power was raised to 19 kW. It was stabilized and held at this level for 77 s after which the power was reduced to 4 kW, in the period lasting for 15 s, simulating the decay heat level. After 170 s the power was turned off, a few seconds later after stopping the water injection.

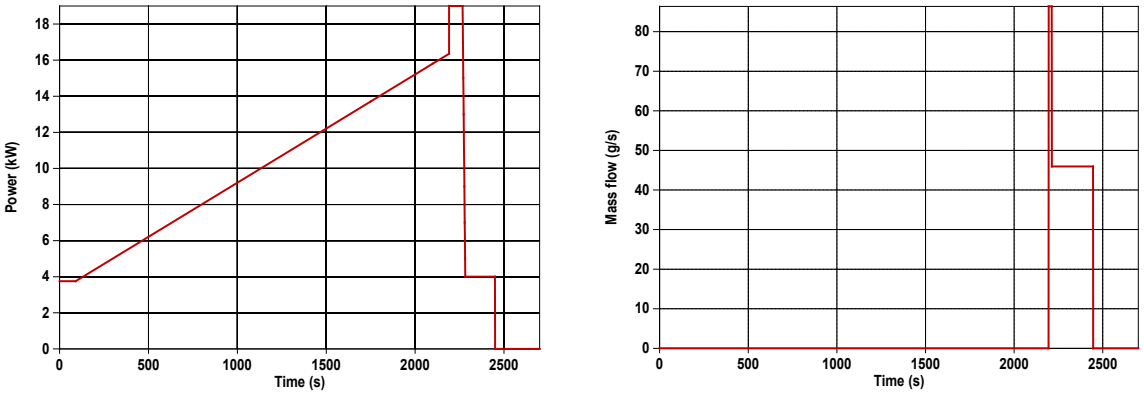

a) b)

Figure 2: a) The electric power supply for the test bundle heating, b) Quench water mass flow rate

3 ASYST COMPUTATION MODEL

3.1 Nodalization

ASYST nodalization of the QUENCH facility is shown in Figure 3. The bundle is divided into 16 thermal hydraulic (TH) volumes (TH component 024), each 0.1 m high. Depending on the test boundary conditions, the flows of argon, steam and water are directed into the bundle from the lower plenum modelled as component 022. The component 026 represents the upper plenum. Components 034 and 040 represent argon and water cooling sections of the inner/outer stainless steel tubes, respectively.

The fuel rod simulators (unheated rod, the inner ring of 8 heated rods, the outer ring of 12 heated rods, 4 corner rods that can be equipped with thermocouples and removed during the experiment to monitor the progress of bundle oxidation and degradation) and the Zircaloy shroud, the tube surrounding the rods, are modelled explicitly as heat structures with two-dimensional heat conduction that can also experience oxidation, fragmentation and melting during a severe accident. The heated zone is covered by axial nodes 4-13 where zirconia insulation is also present. The space above the insulation, between the Zircaloy shroud and the inner stainless steel cylinder is empty, filled with argon. There are high radiative heat losses in that area, modelled as dummy material with time-dependent thermal conductivity. The outer stainless steel tube is modelled as a simple one-dimensional heat conducting structure with temperature boundary conditions. The inside surface of that structure is cooled by argon/water flows, as already mentioned.

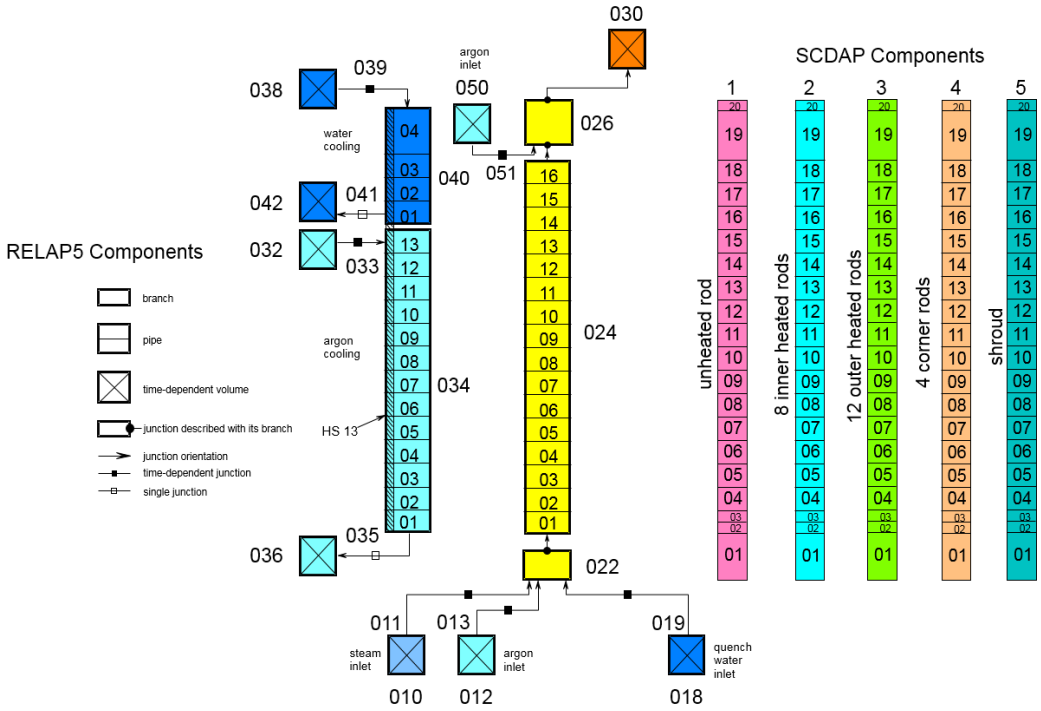

Figure 3: Nodalization of the QUENCH facility used for calculation of QUENCH-02 experiment

3.2 Boundary Conditions and Uncertain Parameters

Uncertain parameters are varied within narrow limits, and are described either by normal or uniform distributions. Their list and description is given in Table 1. The parameters include boundary conditions (steam flow, quench water flow, temperature of the outer stainless steel tube, electrical power), parameters for cladding oxidation, melting and structural behaviour, grid spacer data and cladding geometrical data. Variations in parameters for which there are no strict constraints are described by a normal distribution, while for parameters that are limited either by the design of the facility or boundary conditions, they are described by a uniform distribution.

The number of code runs was 60 (1 base case and 59 calculations with uncertainties). This number of calculations covers 95% of expected outcomes with 95% of probability, as per Wilks' formula [11]. The calculations lasted 2700 s which is in agreement with the duration of the experiment.

Table 1: Input uncertain parameters

Phenomenon	No.	Description	Reference value	Probability density function
Severe accident bundle behaviour (CORE)	1	Temperature for failure of the oxide layer on the outer cladding surface	2500 K	Normal (1.00, 10^{-4})
	2	Fraction of oxidation of the cladding for the stable oxide layer	0.6	Normal (1.00, 10^{-4})
	3	Cladding hoop strain threshold for double-sided oxidation	0.14	Normal (1.00, 10^{-4})
	4	Fraction of cladding surface area covered with drops that results in the blockage that stops local oxidation	0.2	Normal (1.00, 10^{-4})
	5	Surface temperature for freezing of drops of liquefied cladding	1750 K	Normal (1.00, 10^{-4})
	6	Velocity of drops of cladding material slumping down outside the surface of the rod	0.5 m/s	Normal (1.00, 10^{-4})
	7	Rupture strain for the cladding	0.18	Uniform (0.99, 1.01)
	8	Strain for transition from the sausage type cladding deformation to the localized deformation	0.2	Uniform (0.99, 1.01)
	9	Strain limit for the rod-to-rod contact	0.25	Uniform (0.99, 1.01)
	10	Mass of the grid spacer per the rod	$1.6 \cdot 10^{-3}$ kg	Normal (1.00, 10^{-4})
	11	Height of the grid spacer	0.04 m	Normal (1.00, 10^{-4})
	12	Plate thickness of the grid spacer	$0.5 \cdot 10^{-4}$ m	Normal (1.00, 10^{-4})
	13	Radius of the contact area between the grid spacer and the cladding	$1 \cdot 10^{-3}$ m	Normal (1.00, 10^{-4})
	14	Cladding inner radius	$4.65 \cdot 10^{-3}$ m	Uniform (1.00, 1.005)
	15	Cladding outer radius	$5.375 \cdot 10^{-3}$ m	Uniform (1.00, 1.005)
	16	Gas inventory in the simulator rod	$1.391 \cdot 10^{-5}$ kg	Normal (1.00, 10^{-4})
Thermal hydraulic system behaviour (TH)	1	Steam flow	3 g/s	Uniform (0.98, 1.02)
	2	Water flow (reflood)	47-89 g/s	Uniform (0.98, 1.02)
	3	Temperature of the outer stainless steel tube	Experimental measurement (~300-400 K)	Uniform (0.98, 1.02)
Electric heaters (POWER)	-	Electric power of the heaters	Experimental measurement (Figure 2a)	Uniform (0.98, 1.02)

4 CALCULATION OF THE EXPERIMENT

4.1 Results and Discussion

The heating of the bundle is consistent with the electric power profile. Temperature continuously increases from 900 K to 2000 K before the quench phase (Figure 4). In some cases, temperature peaks caused by local oxidation are visible. After the injection of the water and additional increase in power, sudden evaporation, oxidation, temperature rise, melting and damage of the cladding occur. Depending predominantly on the power level, cases with lower power do not experience temperature escalation, quenching is faster, the levels of oxidation and cladding damage are lower. When the power is higher and the injected amount of cold water is lower, the maximum temperature rises above 3000 K. The quench occurs between 2200 s and 2460 s, depending on the scenario. The experiment did not have a pre-oxidation phase because the bundle heating period is terminated before the conditions for oxidation are met (low temperature). This is clearly visible in figure that shows hydrogen generation (Figure 5). About 10% of hydrogen is produced in cases with significant oxidation before the quench phase. Total masses of hydrogen vary from 0.02 kg to 0.33 kg depending on the power, temperature and the amount of steam.

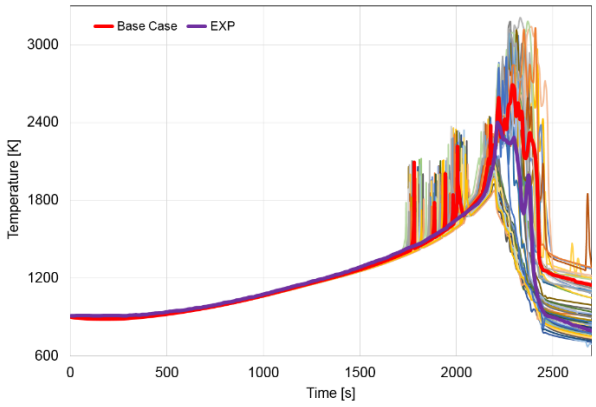

Figure 4: Cladding maximum temperature

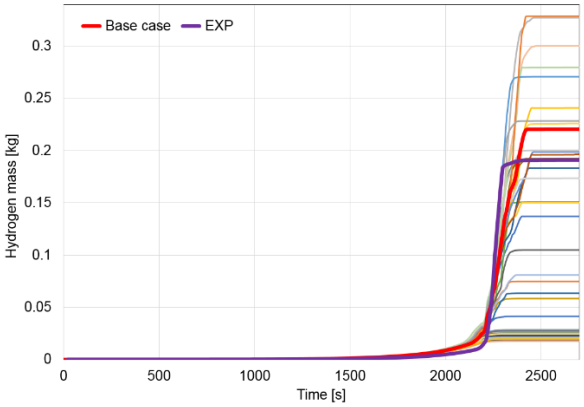

Figure 5: Production of hydrogen

Figure 6 shows collapsed water level in the bundle. The bundle begins to fill with water after initiation of the quench water flow at 2195 s. The water injection is terminated at 2445 s, after which the water level decreases. The results show a pronounced dependence of the water level on the total power, and not on the flow of quench water, whose variations, therefore, do not have much effect on the height of the water inside the bundle. Cases in which the bundle is submerged up to a height of 1 m (the upper limit of the heated part of the rods) experience an earlier quench, while in cases in which the heated part of the bundle is not completely submerged, high temperatures and greater damage to the rods are achieved. Melting and/or cracking of the cladding due to thermal shock, after water injection, caused significant bundle damage in the upper part of the heated segment. The first formations of liquefied material appear at ~2000 s. The timing and intensity of structural damage depend on the temperature, pre-oxidation level and position of rods inside the bundle (radial and axial levels). Some components experienced melting before, and some after the initiation of water injection. For example, in the upper heated part of the central rod, depending on the scenario, 60-80% of the cladding was removed and was later resolidified in the lower, colder zone (Figure 7).

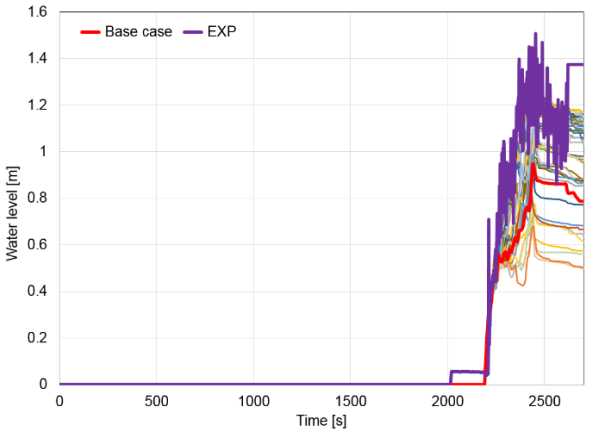

Figure 6: Collapsed water level in the bundle

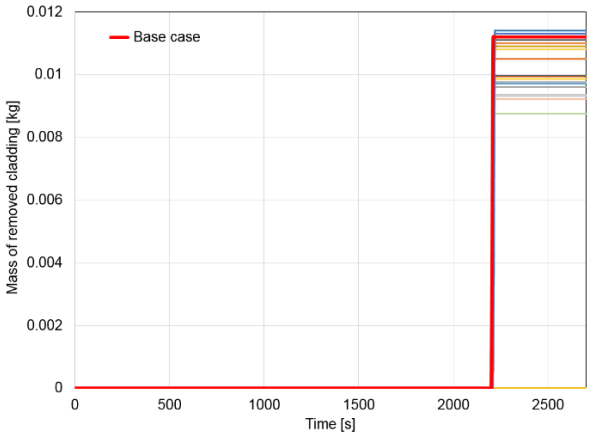

Figure 7: Mass of removed cladding (central rod at ax. level 12)

4.2 Statistical Analysis and Influence Measures

Dispersion of results around the mean value is evaluated using the relative standard deviation (RSD):

$$RSD = \sqrt{\frac{1}{N}\sum_{i=1}^{N}\left(\frac{x_i}{\bar{x}} - 1\right)^2}\,, \tag{1}$$

where N is the sample size, x_i i-th population value, and $\bar{x}$ the population mean.

Relative standard deviations for the maximum cladding temperature (BGMCT), hydrogen generation rate (BGTH), hydrogen production (HYDSUM) and bundle water level (WLEVEL) are shown in Figure 8. Due to a limited local oxidation at 800 s there is a sudden increase of RSD for hydrogen production because it did not happen in all cases. This peak is very pronounced because RSD is relative variable, but actually, the oxidation rate was negligible. Larger deviations between the results of different scenarios occur after the start of water injection. Again, these differences are mostly pronounced for hydrogen production. In the scenarios with a fast quench, the production rate and mass of hydrogen are many times lower than in the scenarios in which there is no quench caused by addition of water, but the temperature drops due to the reduction of electric power.

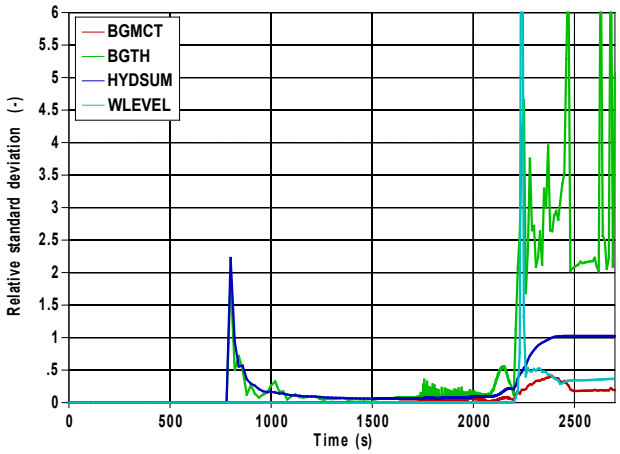

Figure 8: Relative standard deviations for selected output variables

Influence measures are used to assess the correlation between the input uncertain parameters and the output results. One way to quantify this correlation is to calculate the Pearson correlation coefficient:

$$r = \frac{\sum_{i=1}^{N}(x_i - \bar{x})(y_i - \bar{y})}{\sqrt{\sum_{i=1}^{N}(x_i - \bar{x})^2 \sum_{i=1}^{N}(y_i - \bar{y})^2}}, \quad (2)$$

where N is the sample size, x_i, y_i the individual sample points, $\bar{x}$ and $\bar{y}$ sample means.

The influence of selected input parameters, described in Table 1, on the maximum cladding temperature and the hydrogen production is shown in figures 9 and 10, respectively. The most significant input variable is the electric power. There is a strong positive correlation between the power input and the temperature and hydrogen mass. A medium correlation exists between the steam flow and the output variables, but this correlation is negative, meaning that temperature and hydrogen generation rate decrease with increase in steam flow. This is due to the low temperature of the steam that basically cools the bundle and prevents the rise in temperature and the oxidation rate.

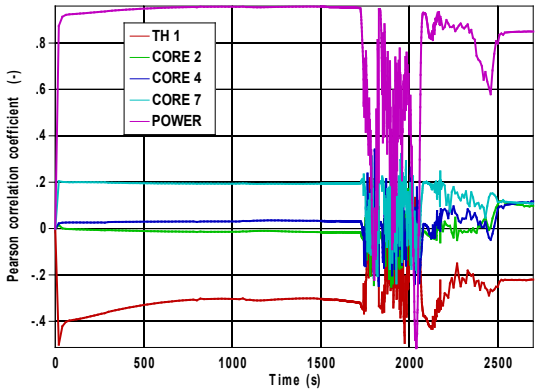

Figure 9: Pearson correlation coefficient between input parameters and the maximum cladding temperature

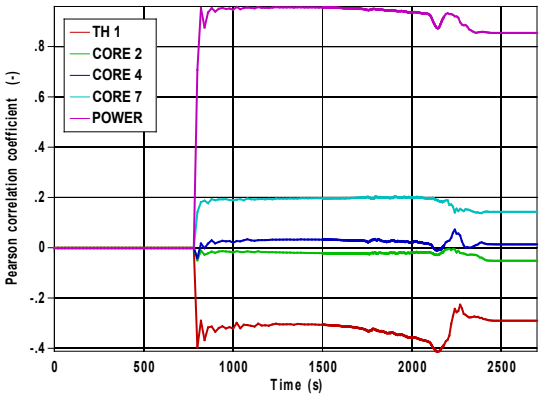

Figure 10: Pearson correlation coefficient between input parameters and the hydrogen production

Additional four cases were calculated to study the influence of electrical power. Using the base case input, the power level was adjusted with the values -2%, -1%, +1%, +2% of the experimental value. As the Pearson correlation coefficient shows, the increase in power causes temperature (Figure 11) and hydrogen production (Figure 12) to increase as well. However, this correlation is not straightforward. Temperature and hydrogen production are higher in the case with a 1% power increase than in the case with a 2% power increase. This can be attributed to a complex bundle/core behaviour during a severe accident sequence and quenching effects (increased oxidation, melting and shattering of the cladding). On the other hand, when the power is reduced by only 1% compared to the base case, the quench occurs almost immediately after the water enters the bundle. The maximum temperature is 800 K lower, and the total hydrogen production is only 10% of the base case value. The reason for this are the lower temperatures of the bundle before the start of the water injection, which were insufficient to induce enhanced evaporation and oxidation, so instead the cooling occurred without noticeable damage and oxidation of the cladding.

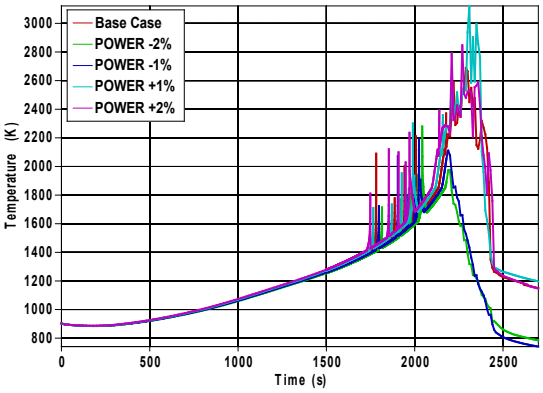

Figure 11: Cladding maximum temperature for different power levels

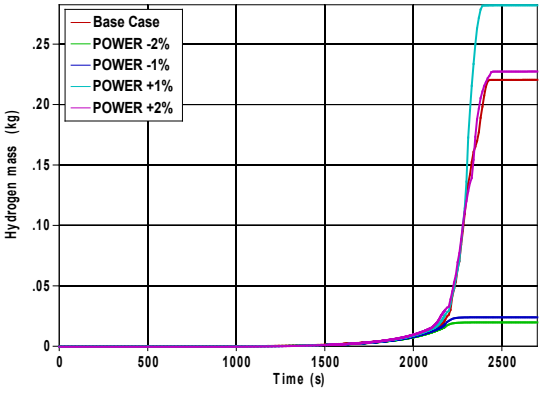

Figure 12: Production of hydrogen for different power levels

5 CONCLUSION

Uncertainties of the experimental initial and boundary conditions and the code parameters related to the fuel rod simulator behaviour during the severe accident have a significant impact on the results. Although the values of uncertain parameters varied within a small interval (+/- 2%), the dispersion of the results was large. The maximum cladding temperature varied between 1900 K and 3200 K, hydrogen production between 0.02 kg and 0.33 kg and the water level in the bundle between 0.5 m and 1.2 m. Such differences occurred after the start of water injection into the bundle, before that the results of different calculations were close. In some calculations the quench occurred instantaneously, while in others it caused cladding damage, increased oxidation and temperature rise.

How sensitive the calculation results are, is best shown by an example of sensitivity analysis for different heater power values. The heater electric power is the most influential parameter determined by the calculation of the Pearson correlation coefficient. Temperature and hydrogen production are higher in the scenario with a smaller power increase (1% compared to 2% increase), while in the scenario with only 1% power reduction compared to the base case, the quench occurs almost immediately after the water is activated, and the total hydrogen production is only 10% of the base value. Another important input parameter is the mass flow rate of steam before the core reflood. While an increase in power causes higher temperature and oxidation, an increase in steam flow leads to a decrease in these variables. The reason is the relatively low temperature of the steam that cools the bundle and prevents the rise in temperature which is necessary to start the oxidation of the Zircaloy alloy.

ACKNOWLEDGMENTS

The authors gratefully express their appreciation to Dr. Chris Allison from Innovative Systems Software for support and cooperation in using the RELAP5/SCDAPSIM and ASYST codes and to Dr. Martin Steinbrück from Karlsruhe Institute of Technology for providing the QUENCH-02 experimental data.

REFERENCES

[1] ASYST THA VER 3 Manuals, Innovative Systems Software, April 2020.

[2] P. Hofmann, C. Homann, W. Leiling, A. Miassoedov, D. Piel, G. Schanz, L. Schmidt, L. Sepold, M. Steinbrueck, "Experimental and Calculational Results of the Experiments. QUENCH-02 and QUENCH-03", Forschungszentrum Karlsruhe, FZKA 6295, July 2000.

[3] G. Schanz, S. Hagen, P. Hofmann, G. Schumacher, L. Sepold, "Information on the evolution of severe LWR fuel element damage obtained in the CORA program", Journal of Nuclear Materials 1992, 188, pp. 131-145, https://doi.org/10.1016/0022-3115(92)90462-T.

[4] S. Šadek, D. Grgić, C. Allison, M. Perez-Ferragut, "Uncertainty Study of the In-Vessel Phase of a Severe Accident in a Pressurized Water Reactor", Energies 2022, 15, 1842. https://doi.org/10.3390/en15051842.

[5] M. Perez, F. Reventos, R. Wagner, C. Allison, "Integrated Uncertainty Analysis using RELAP/SCDAPSIM/MOD4.0", Proc. of the 13th International Topical Meeting on Nuclear Reactor Thermal Hydraulics (NURETH-13), Kanazawa City, Ishikawa Prefecture, Japan, September 27 – October 2, 2009, N13P1252.

[6] A. Nakata, C. M. Allison, J. K. Hohorst, M. Naitoh, K. Matsubara, R. Pericas, "Development and Preliminary Assessment of the new ASYST Integral Analysis BEPU Code using the PBF SFD-ST Bundle Heating and Melting Experiment, a Typical BWR Under Fukushima-Daiichi-Accident-Like Thermal Hydraulic Conditions and PWR for a Steam Line Break in the Containment", Proc. of ICAPP 2021, October 16-20, 2021 (Virtual).

[7] A.K. Trivedi, M. Perez-Ferragut, J.K. Hohorst, C. Allison, "Integrated uncertainty analysis of LBLOCA in AP1000 using RELAP/SCDAPSIM", Proc. of the 12th International Conference of the Croatian Nuclear Society, Zadar, Croatia, 3-6 June, 2018.

[8] C. Allison, B.T. Le, G. Gerova, I. Spasov, M. Perez-Ferragut, J. Hohorst, "QUENCH-06 Experiment Post-Test Calculations and Integrated Uncertainty Analysis With RELAP/SCDAPSIM/MOD3.4 and MOD3.5.", Proc. of the 2018 26th International Conference on Nuclear Engineering, Volume 4: Nuclear Safety, Security, and Cyber Security; Computer Code Verification and Validation, London, England. July 22–26, 2018. V004T15A012. ASME. https://doi.org/10.1115/ICONE26-81912

[9] S. Špalj, S. Šadek, E. Honaiser, "Analysis of International Standard Problem ISP-45 on QUENCH Facility Using RELAP5/SCDAPSIM/MOD3.2 Computer Code", Proc. of the 4th International Conference on Nuclear Option in Countries with Small and Medium Electricity Grids, Dubrovnik, Croatia, 2002.

[10] S. Šadek, N. Debrecin, S. Špalj, "QUENCH-11 Experiment Analysis with RELAP5/SCDAPSIM Code", Proc. of the 7th International Conference on Nuclear Option in Countries with Small and Medium Electricity Grids, Dubrovnik, Croatia, 2008.

[11] S.S. Wilks, "Determination of sample sizes for setting tolerance limits", Ann. Math. Stat. 1941, 12, pp. 91–96.